

Effect of a cap layer on morphological stability of a strained epitaxial film

Hai Liu and Rui Huang^{a)}

Department of Aerospace Engineering and Engineering Mechanics, The University of Texas, Austin, Texas 78712

(Received 1 February 2005; accepted 11 April 2005; published online 7 June 2005)

A strained epitaxial film often undergoes surface roughening during growth and subsequent processes. One possible means to reduce roughening so as to produce an epitaxial film with a flat surface is to deposit an oxide cap layer on the film to suppress the kinetic process of roughening. This paper analyzes the effect of a cap layer on the stability of an epitaxial film and the kinetics of roughening, assuming the interface diffusion between the film and the cap layer as the dominant mechanism of mass transport. A variational principle is formulated, which leads to a nonlinear evolution equation coupled with a boundary-value problem of elasticity. A linear perturbation analysis is then performed, from which the critical wavelength and the fastest growing mode of roughening are obtained. It is found that both the thickness and the residual stress of the cap layer play important roles in controlling the morphological stability and the roughening kinetics. © 2005 American Institute of Physics. [DOI: 10.1063/1.1928311]

I. INTRODUCTION

It is well known that epitaxially deposited films can undergo a transition from layer-by-layer growth to form three-dimensional islands. It has been understood that this transition is due to the presence of elastic stress induced by lattice mismatch between the film and the substrate.^{1–3} While this phenomenon has found important applications as a process to synthesize self-assembled quantum dots for nanoelectronic and optoelectronic devices,⁴ the rough film surface due to the transition is undesired in other applications such as band-gap engineering for microelectronic devices.^{5,6} To improve the film quality, one procedure has been recently proposed to deposit a cap layer on the film at a relatively low temperature to suppress the transition process.⁷ The procedure keeps the epitaxial film at relatively low temperatures, allowing limited relaxation by either surface roughening or dislocation formation. Once the cap layer has been deposited, the film is constrained and thus stabilized during subsequent processes at higher temperatures. Experimental evidence of the cap layer effect has been observed for a Si cap layer on SiGe/SiGeC films⁷ and a ZrO₂ cap on a SiGeC film.⁸ While dislocation formation may still be a concern for film degradation, it may be controlled by several techniques such as strain compensation by carbon incorporation in SiGe alloys.^{9,10}

This paper studies the effects of a cap layer on the stability and kinetics of surface roughening, assuming no dislocation formation. The morphological instability of a stressed solid was first studied by Asaro and Tiller¹¹ and later independently by Srolovitz¹² and Grinfeld.¹³ Following similar ideas, the morphological instability of epitaxial films has been studied by many authors (e.g., Refs. 1–3). It was found that a strained planar film is unstable and the instability is manifested by mass transport mainly via surface diffusion. A

surface chemical potential has been defined^{14,15} and widely used in numerical simulations of nonlinear evolution of surface profiles as well as growth of self-assembled quantum dots.^{16,17} Alternatively, a variational principle based on non-equilibrium thermodynamics provides an equivalent approach, but with a more generic form that can be extended to more complex systems.^{18,19}

The presence of a cap layer on top of a strained epitaxial film has two direct effects on the morphological stability. First, it suppresses the mass transport on the otherwise free surface of the film. Instead, interface diffusion may take place, but typically at a substantially lower rate. Second, the mechanical stiffness of the cap layer tends to stabilize the film. Furthermore, the cap layer is effectively stiffened when subjected to a tensile residual stress, but softened with a compressive residual stress. In fact, a compressive residual stress in the cap layer by itself may cause surface instability, as wrinkling of the oxide scale on an aluminum-containing alloy at high temperatures.^{20,21} To develop a quantitative understanding of these effects, we employ the variational approach to analyze the surface instability and the roughening kinetics of a strained epitaxial film covered by an elastic cap layer.

The rest of the paper is organized as follows. Section II formulates the variational principle, which leads to a nonlinear evolution equation coupled with a boundary-value problem of elasticity. In Sec. III a linear perturbation analysis is performed. The effects of the cap layer on the critical wavelength of perturbation and the fastest growing mode are discussed in Sec. IV. Section V concludes with a summary of the results.

II. FORMULATION

Figure 1 illustrates the model structure of the present study, consisting of a strained epitaxial film sandwiched between a thick substrate and a thin cap layer. The film and the substrate are single crystals and form a coherent interface.

^{a)}Author to whom correspondence should be addressed; Tel: +1-512-471-7558; FAX: +1-512-471-5500; electronic mail: ruihuang@mail.utexas.edu

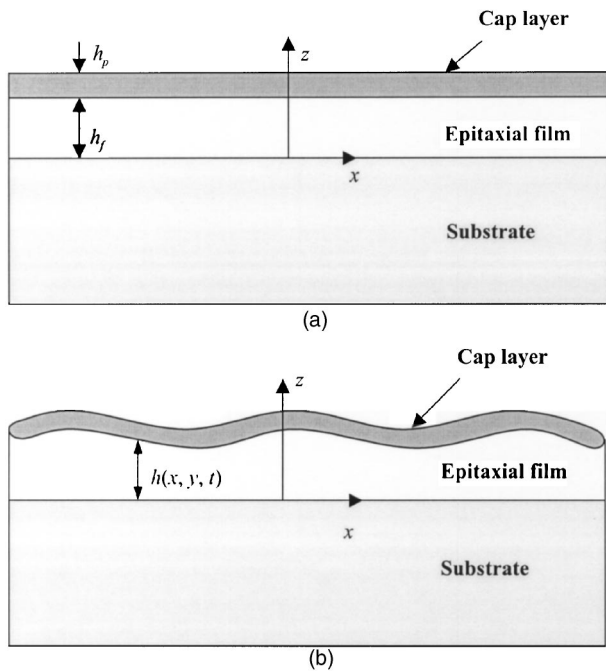


FIG. 1. Schematic of the model structure: (a) the reference state and (b) the state after roughening.

The cap layer, on the other hand, is typically an amorphous oxide. At the reference state [Fig. 1(a)] both the film and the cap layer are flat. The film is subjected to an equibiaxial in-plane strain ε_f due to the lattice mismatch with the substrate, and the cap layer in general is subjected to a biaxial residual strain ε_p ; both strains can be either tensile or compressive, depending on the materials and the deposition processes. The strain energy stored in such a system may be relaxed by various mechanisms.²² This paper considers surface roughening by interface diffusion between the film and the cap layer. A Cartesian coordinate system has been set up in Fig. 1 with the x - y plane coinciding with the film-substrate interface and the z axis as the upward normal of the interface.

A. Energetics

Let $h(x, y)$ represent the profile of the film-cap interface measured from the film-substrate interface. At the reference state, $h(x, y) = h_f$, which is a constant. As the interface roughens, the atoms of the epitaxial film diffuse along the interface, and the cap layer deforms concomitantly. The roughening induces a change to the total free energy (ΔG) of the trilayer system, consisting of the surface/interface energy ($\Delta\Gamma$) and the elastic strain energy in the film (ΔU_f), the substrate (ΔU_s), and the cap layer (ΔU_p), namely,

$$\Delta G = \Delta U_s + \Delta U_f + \Delta U_p + \Delta\Gamma. \quad (1)$$

Consider the elastic energy first. Assume an isotropic, elastic cap layer, modeled as a thin plate undergoing a vertical displacement, $w(x, y)$, relative to the reference state. The strain energy in the cap layer consists of two parts, associated with bending and in-plane deformation,²³ respectively,

$$\Delta U_p = \frac{E_p h_p^3}{24(1-\nu_p^2)} \int_S [(w_{,xx} + w_{,yy})^2 - 2(1-\nu_p)(w_{,xx}w_{,yy} - w_{,xy}^2)] dS + \frac{E_p h_p \varepsilon_p}{2(1-\nu_p)} \int_S (w_{,x}^2 + w_{,y}^2) dS, \quad (2)$$

where h_p is the thickness of the cap layer, E_p is Young's modulus, ν_p is Poisson's ratio, a comma in the subscript denotes partial differentiation with respect to the subsequent variable(s), and S is an arbitrary plane parallel to the flat interface at the reference state. As part of the thin-plate approximation, we have ignored the in-plane displacement of the cap layer.

At the reference state, the strain is uniform in the film and zero in the substrate. Upon roughening, the strain becomes nonuniform in both the film and the substrate. The changes of the respective strain energy are

$$\Delta U_f = \int_S \left(\int_0^h \frac{1}{2} \sigma_{ij}^f \varepsilon_{ij}^f dz - \frac{E_f h_f \varepsilon_f^2}{1-\nu_f} \right) dS, \quad (3)$$

$$\Delta U_s = \frac{1}{2} \int_S \int_0^\infty \sigma_{ij}^s \varepsilon_{ij}^s dz dS, \quad (4)$$

where E_f and ν_f are the Young's modulus and Poisson's ratio of the film, σ_{ij} and ε_{ij} are the stress and strain tensors, and the superscripts f and s denote the film and the substrate, respectively. A repeated Latin subscript (i or j) implies summation over the three coordinates x , y , and z . Both the film and the substrate are assumed to be isotropic in the present study. The nonuniform stress and strain fields must be determined by solving a boundary-value problem as described in a latter section.

Following the thin plate model for the cap layer, the upper and lower faces of the cap layer are assumed to remain parallel. For smooth surfaces with small slope everywhere, the change of the surface energy is approximately

$$\Delta\Gamma = \frac{1}{2}(\gamma_1 + \gamma_2) \int_S (h_{,x}^2 + h_{,y}^2) dS, \quad (5)$$

where γ_1 is the interface energy density of the film-cap interface and γ_2 is the surface energy density of the cap layer. The surface and interface energies are assumed to be isotropic.

B. Variational principle

The change of the total free energy in the model system can be associated with two processes. One is the mass transport, i.e., the atomic diffusion at the film-cap interface for the present study. The divergence of the atomic relocation at the interface results in the change of the interface profile, which leads to, by mass conservation,

$$\delta h = -\Omega \delta l_{\alpha, \alpha}, \quad (6)$$

where Ω is the atomic volume and δl_α is the atomic relocation vector, with α denoting the in-plane coordinate x or y . A repeated Greek subscript implies summation over x and y . The other process is the mechanical displacement in the film

(δu_i^f), the substrate (δu_i^s), and the cap layer (δw). Assuming that the interfaces remain bonded, the compatibility requires that

$$\delta u_i^s = \delta u_i^f \quad (7)$$

at the film–substrate interface ($z=0$), and

$$\delta w = \delta h + \delta u_z^f \quad (8)$$

at the film–cap interface ($z=h$).

Taking the variation of Eqs. (2) to (5), we obtain that

$$\delta \Gamma = -\gamma \int_S \nabla^2 h \delta h \, dS, \quad (9)$$

$$\delta U_p = \int_S (D_p \nabla^4 w - N_p \nabla^2 w) \delta w \, dS, \quad (10)$$

$$\begin{aligned} \delta U_f = & \int_{S_1+S_2} \sigma_{ij}^f \delta u_i^f n_j \, dS - \int_{V_f} \sigma_{ij,j}^f \delta u_i^f \, dV \\ & + \int_{S_1} \frac{1}{2} \sigma_{ij}^f \epsilon_{ij}^f \delta h \, dS, \end{aligned} \quad (11)$$

$$\delta U_s = \int_{S_2} \sigma_{ij}^s \delta u_i^s n_j \, dS - \int_{V_s} \sigma_{ij,j}^s \delta u_i^s \, dV, \quad (12)$$

where $\nabla^2 = \partial^2 / \partial x^2 + \partial^2 / \partial y^2$, $\gamma = \gamma_1 + \gamma_2$, $D_p = E_p h_p^3 / 12(1 - \nu_p^2)$, $N_p = E_p h_p \epsilon_p / (1 - \nu_p)$, $\int_{V_f} (\cdot) \, dV = \int_{V_s} \int_0^h (\cdot) \, dz \, dS$, $\int_{V_s} (\cdot) \, dV = \int_{V_s} \int_{-\infty}^0 (\cdot) \, dz \, dS$, S_1 and S_2 are the film–cap interface and the film–substrate interface, respectively, and n_j is the normal vector of the corresponding interface. Applying the compatibility relations in (7) and (8) leads to the variation of the total free energy

$$\begin{aligned} \delta G = & \int_S \left[D_p \nabla^4 h - (\gamma + N_p) \nabla^2 h + \frac{1}{2} (\sigma_{ij}^f \epsilon_{ij}^f)_{z=h} \right] \delta h \, dS \\ & + \int_S [D_p \nabla^4 h - N_p \nabla^2 h + (\sigma_{3j}^f n_j)_{z=h}] \delta u_z^f \, dS \\ & + \int_S [(\sigma_{\alpha j}^f n_j)_{z=h}] \delta u_\alpha^f \, dS + \int_S [(\sigma_{3j}^f)_{z=0} \\ & - (\sigma_{3j}^s)_{z=0}] \delta u_j \, dS - \int_{V_f} \sigma_{ij,j}^f \delta u_i^f \, dV - \int_{V_s} \sigma_{ij,j}^s \delta u_i^s \, dV \end{aligned} \quad (13)$$

In deriving Eq. (13) we have approximately taken $w \approx h - h_f$ under the assumption of small deformation.

Of the two processes, the mass transport is usually much slower than the mechanical displacement. Consequently, in the time scale of mass transport, it is sufficient to assume that the system maintains mechanical equilibrium. Under this condition, the variational principle dictates that the variation of the free energy vanishes for arbitrary variation in mechanical displacements, which leads to

$$\begin{cases} \sigma_{ij,j}^s = 0 & (V_s) \\ \sigma_{ij,j}^f = 0 & (V_f) \\ \sigma_{3j}^f n_j = -D_p \nabla^4 h + N_p \nabla^2 h & (z=h) \\ \sigma_{\alpha j}^f n_j = 0 & (z=h) \\ \sigma_{3j}^s = \sigma_{3j}^f & (z=0) \end{cases} \quad (14)$$

Equation (14) describes a boundary-value problem for the film–substrate structure subjected to a surface traction due to the cap layer. Together with the constitutive relations for the substrate and the film, the boundary-value problem can be solved to determine the stress and strain fields.

On the other hand, the system is thermodynamically in-equilibrium, as the variation of the free energy with respect to mass transport drives interface diffusion. The thermodynamic driving force P_α is defined as

$$\delta G = - \int_\delta P_\alpha \delta I_\alpha \, dS. \quad (15)$$

By comparing Eqs. (13) and (15) and applying the mechanical equilibrium conditions in Eq. (14) and the mass conservation relation in Eq. (6), we obtain

$$P_\alpha = \Omega \frac{\partial}{\partial x_\alpha} \left\{ D_p \nabla^4 h - (\gamma + N_p) \nabla^2 h + \frac{1}{2} (\sigma_{ij}^f \epsilon_{ij}^f)_{z=h} \right\}. \quad (16)$$

When the cap layer is absent (i.e., $D_p = N_p = 0$), Eq. (16) is reduced to the familiar driving force for surface diffusion, namely, the gradient of the chemical potential at a solid surface.¹⁵ The presence of a cap layer therefore modifies the chemical potential at the interface. A similar driving force was defined for interface diffusion between a strained oxide scale and an aluminum alloy substrate,²⁰ in which the surface energy and the strain energy in the substrate were ignored.

C. Kinetics

The kinetics of interface diffusion is often complex and difficult to characterize experimentally. For simplicity, we assume a linear kinetic law so that the atomic flux rate is proportional to the thermodynamic driving force, namely,

$$J_\alpha = M P_\alpha, \quad (17)$$

where M is a constant characterizing the atomic mobility at the film–cap interface. It is noted that the atomic mobility at an interface strongly depends on the cap layer and is typically smaller than that at a free surface.

The divergence of the atomic flux changes the interface profile, and the mass conservation requires that

$$\frac{\partial h}{\partial t} = -\Omega J_{\alpha,\alpha}. \quad (18)$$

Substitution of Eq. (16) into Eq. (17) and then into Eq. (18) leads to

$$\frac{\partial h}{\partial t} = M \Omega^2 \nabla^2 \left\{ D_p \nabla^4 h - (\gamma + N_p) \nabla^2 h + \frac{1}{2} (\sigma_{ij}^f \epsilon_{ij}^f)_{z=h} \right\}. \quad (19)$$

Equation (19) describes the evolution of the interface profile, which couples with the boundary-value problem described

by Eq. (14). The coupled problem can be solved as follows. At a given instance, the interface profile $h(x, y, t)$ is known. Solve the boundary-value problem to determine the stress and strain at the film–cap interface. Then, substitute the stress and strain into Eq. (19) and integrate over time to update the interface profile. Repeat the procedure to evolve the interface over time. In general, a numerical method is required to solve the boundary-value problem and to integrate the evolution equation. In the following we pursue analytical solutions by a linear perturbation analysis to illustrate the effect of the cap layer.

III. LINEAR PERTURBATION ANALYSIS

An arbitrary interface profile $h(x, y)$ can be represented by the summation of many Fourier components of different wavelengths along different directions. For linear perturbation analysis, we consider a single component, i.e., a sinusoidal perturbation with a constant wavelength. Since the model structure is isotropic in the x - y plane, any direction of the sinusoidal wave is equivalent, and we choose the direction to coincide with the x coordinate without losing any generality. Thus, we write

$$h(x, t) = h_f + A(t) \sin kx, \quad (20)$$

where A is the perturbation amplitude and k is the wave number.

The perturbation induces the change of the stress and strain fields in the film and the substrate, which can be determined by two steps considering the effects of mass relocation and the interaction with the cap layer separately. First, assuming no cap layer, the mass relocation at the surface of the film changes the morphology. The associated change in the stress field can be obtained by solving an equivalent problem with a distributed shear traction acting on the surface of a flat film, as described in Ref. 2. The corresponding shear traction is proportional to the slope of the surface, namely,

$$\sigma_{zx}(z = h_f) = \frac{E_f \varepsilon_f}{1 - \nu_f} k A \cos kx. \quad (21)$$

Next, the cap layer upon deflection exerts a normal traction on the surface of the film, i.e.,

$$\sigma_{zz}(z = h_f) = -D_p \nabla^4 h + N_p \nabla^2 h. \quad (22)$$

Substituting Eq. (20) into Eq. (22), we obtain

$$\sigma_{zz}(z = h_f) = (-D_p k^4 - N_p k^2) A \sin kx. \quad (23)$$

Equations (21) and (23) represent the linear approximation of the boundary conditions at the film surface ($z = h$) in Eq. (14) for small perturbations.

The solution to the boundary-value problem is given in the Appendix. In particular, under the shear and normal tractions in Eqs. (21) and (23), the in-plane displacement at the film surface is

$$u_x^f(z = h_f) = \frac{1 + \nu_f}{E_f} \left[\beta_1 \frac{E_f \varepsilon_f}{1 - \nu_f} - \beta_2 (D_p k^3 + N_p k) \right] A \cos(kx), \quad (24)$$

where β_1 and β_2 are given in Eqs. (A18) and (A19).

For a small perturbation from the reference state, Eq. (19) is reduced to

$$\frac{\partial h}{\partial t} = M \Omega^2 \nabla^2 \left\{ D_p \nabla^4 h - (\gamma + N_p) \nabla^2 h + \frac{E_f \varepsilon_f}{1 - \nu_f} \left(\frac{\partial u_z^f}{\partial x} \right)_{z=h_f} \right\}. \quad (25)$$

Substitution of Eqs. (20) and (24) into Eq. (25) leads to

$$\frac{dA}{dt} = \alpha A, \quad (26)$$

where

$$\alpha = M \Omega^2 k^2 \left\{ \frac{1 + \nu}{(1 - \nu)^2} \beta_1 E_f \varepsilon_f^2 k - \left[1 + \left(1 + \frac{1 + \nu}{1 - \nu} \varepsilon_f \beta_2 \right) \frac{N_p}{\gamma} \right] \gamma k^2 - \left(1 + \frac{1 + \nu}{1 - \nu} \varepsilon_f \beta_2 \right) D_p k^4 \right\}. \quad (27)$$

Therefore, the amplitude of the perturbation as a function of time is $A(t) = A_0 \exp(\alpha t)$, where A_0 is the initial amplitude. The perturbation either grows or decays, depending on the sign of α . The first term in the bracket of Eq. (27) is positive for both tensile and compressive film strain ε_f , which drives roughening to relax the strain energy. The second term represents the penalty due to the increase of surface energy and, in addition, the stretching of the cap layer. The residual strain in the cap layer can be either stabilizing ($N_p > 0$) or destabilizing ($N_p < 0$), depending on its sign. The third term further penalizes the roughening due to the flexural stiffness of the cap layer. The competition among the three terms leads to two length scales. A comparison between the first two terms defines a length

$$l_1 = \frac{\gamma E_f}{(1 + \nu) \sigma_0^2}, \quad (28)$$

where σ_0 is the biaxial film stress at the reference state, i.e., $\sigma_0 = E_f \varepsilon_f / (1 - \nu)$. This length scale has been used previously to characterize the competition between the surface energy and the strain energy. Similarly, a comparison between the first and the third term leads to another length

$$l_2 = \left[\frac{E_f D_p}{(1 + \nu) \sigma_0^2} \right]^{1/3}, \quad (29)$$

which characterizes the effect of the bending stiffness of the cap layer.

Rewrite Eq. (27) with the lengths l_1 and l_2 as

$$\alpha = \frac{1}{\tau} (kl_1)^3 [\beta_1 - (1 + \xi_1)kl_1 - \xi_2(kl_2)^3], \quad (30)$$

where

$$\xi_1 = \left(1 + \frac{1+v}{1-v} \varepsilon_f \beta_2 \right) \frac{N_D}{\gamma}, \quad (31)$$

$$\xi_2 = 1 + \frac{1+v}{1-v} \varepsilon_f \beta_2, \quad (32)$$

$$\tau = \frac{\gamma^3 E_f^4}{(1+v)^4 M \Omega^2 \sigma_0^8}. \quad (33)$$

The parameter ξ_1 can be either positive or negative, characterizing the effect of the residual stress in the cap layer. Equation (33) defines a time scale for the evolution process, which is identical to the time scale for the evolution of a free surface,^{1,2} except that the atomic mobility at the interface for the present case is typically much smaller. Note that, while Eq. (30) appears to take a polynomial form in terms of the wave number k , the actual dependence of the growth rate on the wave number is more complicated since the parameters β_1 and β_2 are, in general, functions of the wave number as given in Eqs. (A18) and (A19). The effect of the elastic stiffness of the substrate is also included through the definitions of β_1 and β_2 .

IV. RESULTS AND DISCUSSIONS

Compared to the previous studies on films with no cap layer, Eq. (30) apparently includes two additional terms that represent the effect of the cap layer. To make the discussion more concrete, we consider a specific system with an epitaxial $\text{Si}_{0.5}\text{Ge}_{0.5}$ film sandwiched between a $\text{Si}(100)$ substrate and a SiO_2 cap layer. The Young's modulus of $\text{Si}_{0.5}\text{Ge}_{0.5}$ and Si are 116 and 130 GPa, respectively. The Poisson's ratio is taken to be 0.25 for both the film and the substrate. The mismatch strain in the film is -0.02 . The cap layer has a Young's modulus of 71 GPa and a Poisson's ratio of 0.16. Various thickness and residual stresses in the cap layer will be considered. Taking a typical value of 1 J/m^2 for the surface energy density γ , the length scale l_1 defined in Eq. (28) is then 9.7 nm. The other length scale l_2 is proportional to the thickness of the cap layer, $l_2 = 3.89h_p$ for the present system. The time scale defined in Eq. (33), however, is more difficult to estimate due to the uncertainty of the atomic mobility at the interface. Roughly, the time scale strongly depends on the temperature and is significantly longer than that for the evolution of a free surface.

Figure 2 plots the normalized growth rate $\alpha\tau$ as a function of the wave number kl_1 with and without a cap layer. As noted in previous studies, without a cap layer ($h_p=0$), the flat film is unstable; there exists a critical wave number, below which the perturbation grows. The presence of a cap layer with no residual stress tends to stabilize the film, leading to a smaller critical wave number (longer wavelength) and a slower growth rate. Both the critical wave number and the

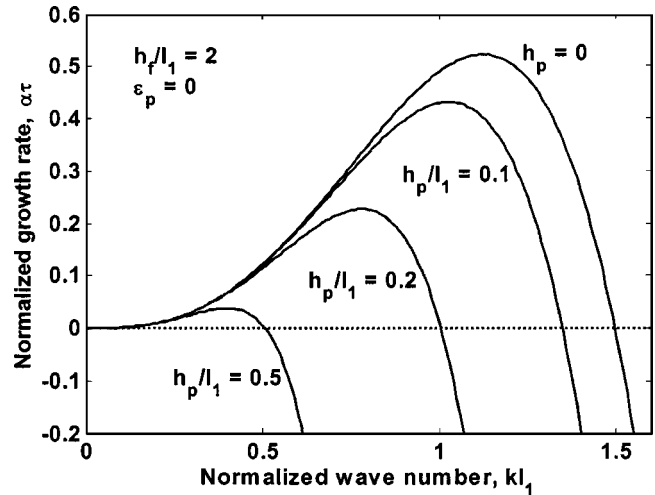


FIG. 2. Normalized growth rate as a function of the wave number with and without a cap layer.

growth rate decrease as the thickness of the cap layer increases. The system, however, remains unstable at the long wavelength end.

The critical wave number also depends on the film thickness and the stiffness of the substrate, as shown in Fig. 3 for the case with no cap layer. Similar plots were reported previously.^{1,2} Two points are noted here. First, for a given stiffness ratio, the critical wavelength is bounded between two limits. For thick films ($h_f/l_1 > 3$) the effect of the substrate is negligible, and the critical wavelength approaches that for a stressed solid in the half plane, which is

$$\lambda_\infty = \frac{\pi}{1-v} l_1. \quad (34)$$

On the other hand, for very thin films ($h_f/l_1 \rightarrow 0$) the substrate effect dominates, and the critical wavelength again approaches that for a stressed half plane but now with the substrate stiffness, i.e.,

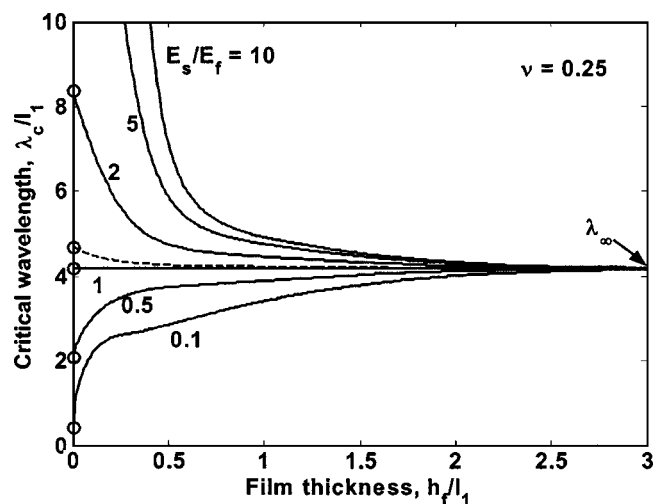


FIG. 3. The critical wavelength as a function of the film thickness for various stiffness ratios between the substrate and the film (with no cap layer). The dashed line is for a $\text{Si}_{0.5}\text{Ge}_{0.5}$ film on a $\text{Si}(100)$ substrate. The open circles are the solution for limiting cases with very thin films.

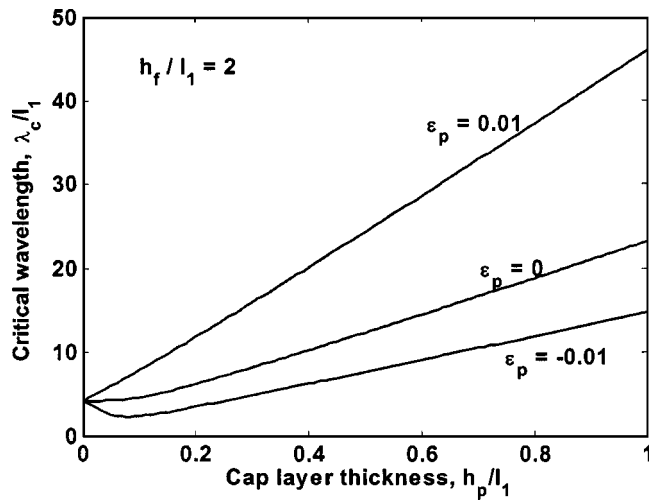


FIG. 4. Effect of an elastic cap layer on the critical wavelength.

$$\lambda_0 = \frac{\pi}{1 - \nu} \frac{E_s}{E_f} l_1, \quad (35)$$

as denoted by the open circles in Fig. 3 for various stiffness ratios. For an arbitrary film thickness, the critical wavelength is in between. When the substrate and the film have the same stiffness, the critical wavelength is independent of the film thickness. For SiGe films on Si substrates, the stiffness ratio is close to unity and the critical wavelength weakly depends on the film thickness, as shown by the dashed line in Fig. 3 for a $\text{Si}_{0.5}\text{Ge}_{0.5}$ film. The second point to note is that a stiffer substrate significantly increases the critical wavelength for thin films ($h_f/l_1 < 1$). At the limit of a rigid substrate, the critical wavelength approaches infinity for the film below a critical thickness. These results agree with previous studies.^{1,2}

The effect of the cap layer on the critical wavelength is shown in Fig. 4. With no residual stress, the flexural stiffness of the cap layer disfavors roughening. Consequently, the critical wavelength increases with the thickness of the cap layer. A tensile residual stress ($\epsilon_p > 0$) in the cap layer further stiffens the layer against roughening, leading to a significantly longer critical wavelength. The epitaxial film is therefore effectively stabilized. On the other hand, a compressive residual stress ($\epsilon_p < 0$) destabilizes the film because roughening relaxes the compressive stress in the cap layer. This leads to a shorter critical wavelength for a thin cap layer. However, as the thickness of the cap layer increases, the stabilizing effect due to the flexural stiffness eventually overcomes the destabilizing effect due to compression, and the critical wavelength then increases. Therefore, a minimum thickness is required for a compressively stressed cap layer to stabilize the epitaxial film.

Figure 2 shows that the cap layer significantly affects the kinetics of surface roughening. At the initial stage of roughening, the fastest growing mode dominates. Both the wavelength and the growth rate of the fastest growing mode are influenced by the cap layer. Generally speaking, the wavelength increases and the growth rate decreases with the cap layer, as shown in Fig. 5. In fact, the cap layer suppresses the kinetic process of roughening. Recall that interface diffusion

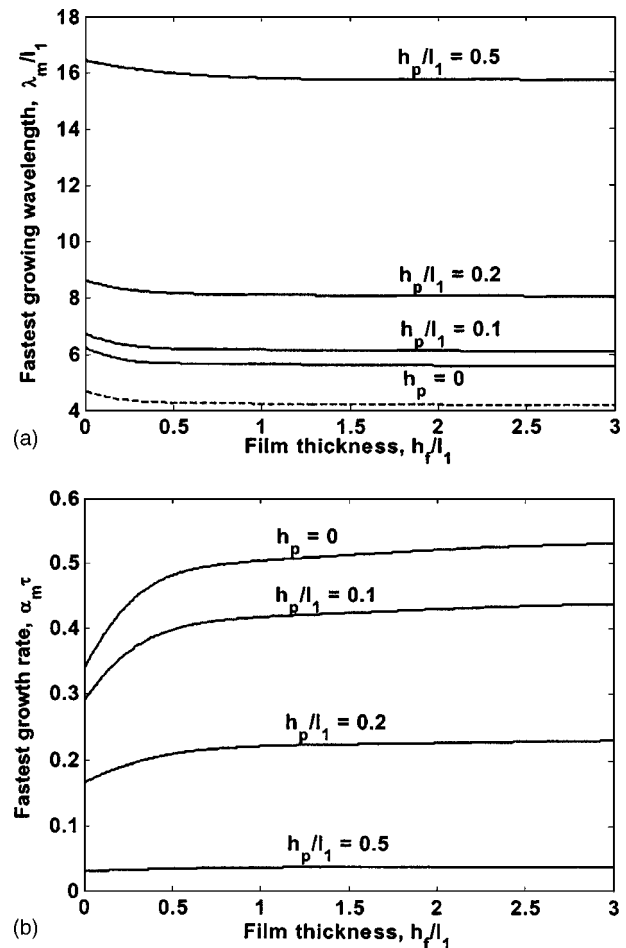


FIG. 5. (a) The wavelength and (b) the growth rate of the fastest growing mode as functions of the film thickness with and without a cap layer. The dashed line in (a) is the critical wavelength with no cap layer.

is typically much slower than surface diffusion, and therefore the effect of the cap layer on the growth rate is even more substantial. The residual stress in the cap layer also has a strong effect on the kinetics, as illustrated in Fig. 6. A tensile stress enhances the stabilizing effect of the cap layer, leading to longer wavelengths and slower growth rate. A compressive stress, however, destabilizes the system, leading to shorter wavelengths and faster growth rate. This is not surprising because a compressed cap layer by itself tends to buckle to relax the compressive stress. The competition between the compressive residual stress and the stiffness of the cap layer leads to a minimum wavelength and a maximum growth rate at a specific cap layer thickness. Therefore, care must be taken to determine the thickness when using a compressively stressed cap layer to stabilize the epitaxial film.

V. SUMMARY

In this paper, a variational approach is formulated to analyze the effect of a cap layer on morphological stability and roughening kinetics of a strained epitaxial film. Atomic diffusion at the film–cap interface is considered. The thermodynamic driving force is defined with the presence of the cap layer. The derived evolution equation couples with a boundary-value problem of elasticity. A linear perturbation

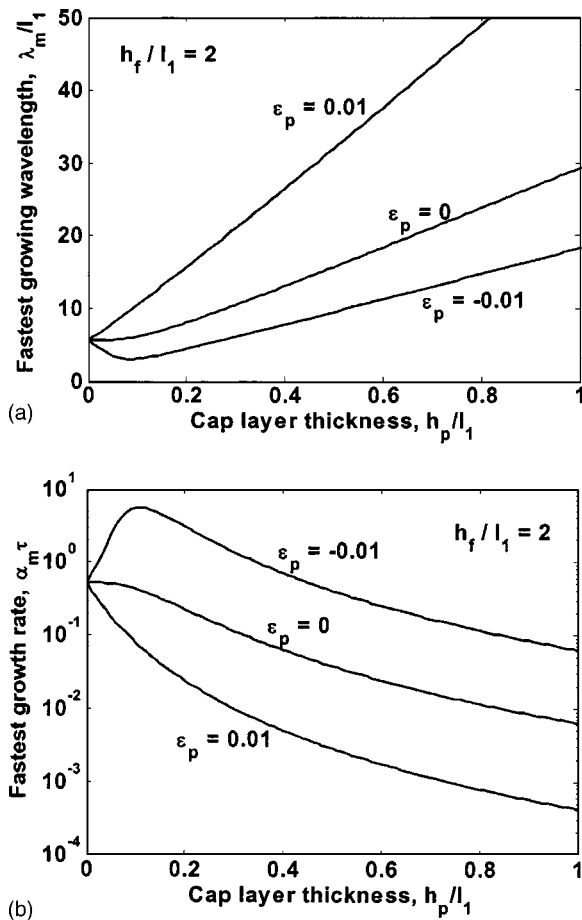


FIG. 6. (a) The wavelength and (b) the growth rate of the fastest growing mode as functions of the cap layer thickness.

analysis is then performed, based on which the effect of the cap layer is discussed. The flexural stiffness, which scales with the cube of its thickness, tends to stabilize the film, leading to longer critical wavelengths and lower growth rate. A tensile residual stress in the cap layer further enhances the stabilizing effect. A compressive residual stress, however, destabilizes the film. It is suggested that the thickness be carefully selected when using a compressively stressed cap layer to stabilize the epitaxial film.

ACKNOWLEDGMENTS

The authors are grateful for the support by NSF Grant No. CMS-0412851 and the Texas Advanced Materials Research Center. R.H. thanks Professor S. K. Banerjee for helpful discussions.

APPENDIX

Consider a flat elastic film of thickness h_f on an infinitely thick elastic substrate subjected to a periodic traction (normal and shear) on the surface. The plane strain problem can be solved by using the stress and displacement potentials.²⁴ The stress components and the displacements in the film are

$$\sigma_{xx}^f = \{C_1 \cosh(kz) + C_2 \sinh(kz) + C_3[2 \sinh(kz) + kz \cosh(kz)] + C_4[2 \cosh(kz) + kz \sinh(kz)]\} \sin kx, \quad (\text{A1})$$

$$\sigma_{zz}^f = -[C_1 \cosh(kz) + C_2 \sinh(kz) + C_3 kz \cosh(kz) + C_4 kz \sinh(kz)] \sin kx, \quad (\text{A2})$$

$$\sigma_{zx}^f = -\{C_1 \sinh(kz) + C_2 \cosh(kz) + C_3[\cosh(kz) + kz \sinh(kz)] + C_4[\sinh(kz) + kz \cosh(kz)]\} \cos kx, \quad (\text{A3})$$

$$u_x^f = -\frac{1+v_f}{E_f k} \left(\begin{array}{l} C_1 \cosh(kz) + C_2 \sinh(kz) \\ + C_3[kz \cosh(kz) + 2(1-\nu) \sinh(kz)] \\ + C_4[kz \sinh(kz) + 2(1-\nu) \cosh(kz)] \end{array} \right) \cos kx, \quad (\text{A4})$$

$$u_z^f = -\frac{1+v_f}{E_f k} \left(\begin{array}{l} C_1 \sinh(kz) + C_2 \cosh(kz) \\ + C_3[(2\nu-1) \cosh(kz) + kz \sinh(kz)] \\ + C_4[(2\nu-1) \sinh(kz) + kz \cosh(kz)] \end{array} \right) \sin kx. \quad (\text{A5})$$

For the substrate of infinite thickness ($0 > z > -\infty$), the solution is reduced to

$$\sigma_{xx}^s = [D_1 + D_2(2 + kz)] \exp(kz) \sin kx, \quad (\text{A6})$$

$$\sigma_{zz}^s = -[D_1 + D_2 kz] \exp(kz) \sin kx, \quad (\text{A7})$$

$$\sigma_{zx}^s = -[D_1 + D_2(1 + kz)] \exp(kz) \cos kx, \quad (\text{A8})$$

$$u_x^s = -\frac{1+\nu_s}{E_s k} [D_1 + D_2(2 - 2\nu + kz)] \exp(kz) \cos kx, \quad (\text{A9})$$

$$u_z^s = -\frac{1+\nu_s}{E_s k} [D_1 - D_2(1 - 2\nu - kz)] \exp(kz) \sin kx. \quad (\text{A10})$$

The six coefficients are determined by the boundary conditions at the film surface ($z=h_f$) and the continuity conditions at the film-substrate interface ($z=0$), i.e.,

$$\sigma_{zx}^f(z=h_f) = B_1 \cos kx, \quad (\text{A11})$$

$$\sigma_{zz}^f(z=h_f) = B_2 \sin kx, \quad (\text{A12})$$

$$\sigma_{zx}^f(z=0) = \sigma_{zx}^s(z=0), \quad (\text{A13})$$

$$\sigma_{zz}^f(z=0) = \sigma_{zz}^s(z=0), \quad (\text{A14})$$

$$u_x^f(z=0) = u_x^s(z=0), \quad (\text{A15})$$

$$u_z^f(z=0) = u_z^s(z=0), \quad (\text{A16})$$

where B_1 and B_2 are the amplitudes of the shear and normal tractions acting on the surface, respectively.

After obtaining the coefficients, the displacements at the film surface can be determined. In particular, the shear displacement at the surface is given by

$$u_x^f(x, z = h_f) = \frac{1+v}{E_f k} [\beta_1 B_1 + \beta_2 B_2] \cos kx, \quad (\text{A17})$$

where

$$\beta_2 = \frac{(2\nu-1)s_2 \cosh(2kh_f) + (2\nu-1)s_3 \sinh(2kh_f) + s_4(kh_f)^2 + s_5}{s_1 + s_2 \cosh(2kh_f) + s_3 \sinh(2kh_f) + s_4(kh_f)^2}, \quad (\text{A19})$$

and

$$\begin{aligned} s_1 &= (p-1)[3-4\nu+p(8\nu^2-12\nu+5)], \\ s_2 &= (1+p^2)(3-4\nu)+2p(1-2\nu)^2, \\ s_3 &= 8p(1-\nu)^2, \\ s_4 &= 2(p-1)(p+3-4\nu), \\ s_5 &= (p-1)^2(3-4\nu)(1-2\nu), \end{aligned} \quad (\text{A20})$$

with $p = E_s/E_f$. In the above solution we have assumed $\nu_s = \nu_f = \nu$ to simplify the result.

The above solution can be reduced in several limiting cases. First, for a rigid substrate (i.e., $p \rightarrow \infty$), (A18) and (A19) are reduced to

$$\beta_1 = (1-\nu) \frac{(3-4\nu)\sinh(2kh_f) + 2kh_f}{(3-4\nu)\cosh^2(kh_f) + (kh_f)^2 + (2\nu-1)^2}, \quad (\text{A21})$$

$$\beta_2 = \frac{(3-4\nu)(2\nu-1)\sinh^2(kh_f) + (kh_f)^2}{(3-4\nu)\cosh^2(kh_f) + (kh_f)^2 + (2\nu-1)^2}, \quad (\text{A22})$$

which are identical to the solution for an elastic layer with a fixed boundary at the bottom given in Ref. 24. The solution may be further reduced for incompressible materials ($\nu = 0.5$). At the opposite limit when the substrate stiffness is approaching zero ($p \rightarrow 0$), we have

$$\beta_1 = (1-\nu) \frac{\sinh(2kh_f) - 2kh_f}{\sinh^2(kh_f) - (kh_f)^2}, \quad (\text{A23})$$

$$\beta_2 = \frac{(2\nu-1)\sinh^2(kh_f) - (kh_f)^2}{\sinh^2(kh_f) - (kh_f)^2}, \quad (\text{A24})$$

which corresponds to the solution for an elastic layer with no substrate constraint, i.e., a traction-free surface at the bottom.

For an infinitely thick elastic film (i.e., $kh_f \rightarrow \infty$), the solution is independent of the substrate and Eq. (A17) reduces to

$$\beta_1 = \frac{2(1-\nu)[s_2 \sinh(2kh_f) + s_3 \cosh(2kh_f) + s_4 kh_f]}{s_1 + s_2 \cosh(2kh_f) + s_3 \sinh(2kh_f) + s_4(kh_f)^2}, \quad (\text{A18})$$

$$u_x = \frac{1+v}{E_f k} [2(1-\nu)B_1 + (2\nu-1)B_2] \cos kx, \quad (\text{A25})$$

which is the solution for an elastic half plane.¹¹ In the other limit when the elastic film is very thin (i.e., $kh_f \rightarrow 0$), the solution is reduced to

$$u_x = \frac{1+v}{E_s k} [2(1-\nu)B_1 + (2\nu-1)B_2] \cos kx, \quad (\text{A26})$$

which is again the solution for an elastic half plane, but now with the substrate's stiffness. The two solutions, therefore, bound the general solution for elastic films of arbitrary thickness. In the special case when the film and the substrate have the same elastic modulus (i.e., $p=1$), the two bounds collapse and the solution is independent of the thickness.

¹B. J. Spencer, P. W. Voorhees, and S. H. Davis, Phys. Rev. Lett. **67**, 3696 (1991).

²L. B. Freund and F. Jonstottir, J. Mech. Phys. Solids **41**, 1245 (1993).

³H. Gao and W. D. Nix, Annu. Rev. Mater. Sci. **29**, 173 (1999).

⁴B. Yang, F. Liu, and M. G. Lagally, Phys. Rev. Lett. **92**, 025502 (2004).

⁵M. Yang, J. C. Sturm, and J. Prevost, Phys. Rev. B **56**, 1973 (1997).

⁶Z. H. Shi, D. Onsongo, and S. K. Banerjee, Appl. Surf. Sci. **224**, 248 (2004).

⁷G. S. Kar, A. Dhar, L. K. Bera, S. K. Ray, S. John, and S. K. Banerjee, J. Mater. Sci.: Mater. Electron. **13**, 49 (2002).

⁸R. Mahapatra, S. Maikap, J.-H. Lee, G. S. Kar, A. Dhar, D.-Y. Kim, D. Bhattacharya, and S. K. Ray, J. Vac. Sci. Technol. A **21**, 1758 (2003).

⁹H. J. Osten, Mater. Sci. Eng., B **36**, 268 (1996).

¹⁰A. C. Mocuta and D. W. Greve, J. Vac. Sci. Technol. A **17**, 1239 (1999).

¹¹R. J. Asaro and W. A. Tiller, Metall. Trans. **3**, 1789 (1972).

¹²D. J. Srolovitz, Acta Metall. **37**, 621 (1989).

¹³M. A. Grinfeld, J. Nonlinear Sci. **3**, 35 (1993).

¹⁴C. H. Wu, J. Mech. Phys. Solids **44**, 2059 (1996).

¹⁵L. B. Freund, J. Mech. Phys. Solids **46**, 1835 (1998).

¹⁶Y. W. Zhang and A. F. Bower, J. Mech. Phys. Solids **47**, 2273 (1999).

¹⁷C.-H. Chiu, Appl. Phys. Lett. **75**, 3473 (1999).

¹⁸A. C. F. Cocks and S. P. A. Gill, Acta Mater. **44**, 4765 (1996).

¹⁹Z. Suo, Adv. Appl. Mech. **33**, 193 (1997).

²⁰Z. Suo, J. Mech. Phys. Solids **43**, 829 (1995).

²¹V. K. Tolpygo and D. R. Clarke, Acta Mater. **46**, 5153 (1998).

²²J. Tersoff and F. K. LeGoues, Phys. Rev. Lett. **72**, 3570 (1994).

²³S. Timoshenko and S. Woinowsky-Krieger, *Theory of Plates and Shells*, 2nd ed. (McGraw-Hill, New York, 1987).

²⁴R. Huang, J. Mech. Phys. Solids **53**, 63 (2005).